UDC 539.4

Preparation, Modeling, and Optimization of Mechanical Properties of Epoxy/HIPS/Silica Hybrid Nanocomposite Using Combination of Central Composite Design and Genetic Algorithm. Part 2. Studies on Flexural, Compression, and Impact Strength

Y. Rostamiyan,[a,1] A. B. Fereidoon,[a] A. Omrani,[b] and D. D. Ganji[c]

[a] Semnan University, Semnan, Iran

[b] University of Mazandaran, Babolsar, Iran

[c] Babol University of Technology, Babol, Iran

[1] y.rostamiyan@yahoo.com

УДК 539.4

Компоновка, моделирование и оптимизация механических свойств гибридного нанокомпозита из эпоксидной смолы, ударопрочного полистирола и кремнезема с использованием центрального композиционного плана и генетического алгоритма. Сообщение 2. Исследования прочности при изгибе и сжатии и ударной вязкости

Я. Ростамиян[а], А. Б. Ферейдун[а], А. Омрани[б], Д. Д. Ганжи[в]

[а] Университет г. Семнан, Иран

[б] Университет Мазендерана, Бабольсер, Иран

[в] Технологический университет г. Баболь, Иран

Несмотря на то что эпоксидные смолы обладают высоким пределом прочности при растяжении, они хрупкие и характеризуются слабым сопротивлением развитию трещины. С целью улучшения механической прочности и вязкости разрушения эпоксидных нанокомпозитов в качестве модификатора использовали новый комбинированный термопластичный дисперсный нанонаполнитель. Полученный трехкомпонентный эпоксидный нанокомпозит содержит ударопрочный полистирол в виде термопластичных и кремнеземных наночастиц, представляющих его дисперсные фазы. Чтобы получить более высокие показатели прочности без воздействия на другие заданные механические показатели, проводили испытания на прочность при изгибе и сжатии и на ударную вязкость. Для представления математических моделей с целью прогнозирования механического поведения гибридного нанокомпозита в качестве функции физических факторов использовали центральный композиционный план. Исследовали содержание ударопрочного полистирола, кремнезема и упрочняющего элемента в нанокомпозите. На основе математических функций, полученных по модели центрального композиционного плана, для выведения оптимальных значений механических свойств использовали генетический алгоритм, являющийся одним из самых мощных средств оптимизации. Установлено, что сочетание наночастиц на основе ударопрочного полистирола и кремнезема значительно увеличивает сопротивление эпоксидной смолы сжатию и удару на 57 и 421% соответственно. При сопротивлении изгибу положительных изменений не наблюдается, удлинение при изгибном разрыве увеличивается до 144%. С помощью энергодисперсионного рентгеновского излучения и сканирующей электронной микроскопии проведено исследование морфологии поверхности разрушения.

Ключевые слова: эпоксидная смола, вязкость разрушения, ударопрочный полистирол, кремнезем, механические свойства, центральный композиционный план, генетический алгоритм.

Introduction. Epoxy polymer is one the most applicable polymeric matrices used for reinforced composite materials [1–3]. Owing to amorphous and highly crosslinked structure, epoxy polymer has become an exclusive material with unique properties such as high modulus and failure strength, low creep and reliable performance at elevated temperatures [4]. Despite the mentioned desired characteristics, poor resistance to crack nucleation and growth, as well as brittleness, are the blind spots of epoxy materials [4]. For many years, incorporation of microphase dispersed rubber [5–7] or different thermoplastic polymers [8, 9] was one of the well-known methods to increase impact strength of thermoset epoxy polymers. Due to its minor effect on other desired mechanical properties, toughening with engineering thermoplastics, such as polysulfone [10], polyetheramide [11], ABS [12], and polyethersulfone [13] is also rather effective. As a rule, rubber or thermoplastics present in epoxy resin can be of importance in improving the fracture toughness, but on the other hand, they cause higher viscosity and dramatically decrease the strength, elastic modulus and stiffness [14–17]. It has also been proposed to increase toughness and stiffhess with glass or ceramic-based rigid inorganic particles of a 4-100-μm diameter [18, 19].

It is noteworthy that since these particles are large, the viscosity of epoxy resin increases which complicates the production process to some extent [4]. In the last decade, the employment of nanostruclures in pohymer matrices to improve such mechanical properties as tensile, compression, and flexural strength values, has created new potentials, in comparison with traditional composite materials [4]. Nanoparticles (e.g., silica) due to their small size, do not exert noticeable influence on the composition viscosity [20]. It should be noted that the difference between nano- and microparticles is mainlyin their high specific surface [21–23]. Previous studies demonstrated that addition of relatively low-cost nanosilica to the epoxy matrix may considerably improve mechanical properlies [4, 24]. It is noteworthy that although the addition of nanoparticles may have a significant effect on some mechanical properties, it does not greatly influence the impact strength improvement of epoxy-based composites. Some researchers also showed that the addition of soft particles and rigid fillers to epoxy resin as a hybrid composite enhanced its strength and fracture toughness. For example, the addition of micron-sized glass spheres together with rubber particles to epoxy matrices exhibited a synergistic toughening effect with acceptable strength enhancement [25, 26]. To study the mechanical properties of a hybrid epoxy-based nanocomposite, effective quantitive factors should be introduced. It can be found in many previous studies [27–29] that the weight percentage of reinforcing toughening agent and nanofiller are the most critical parameters, which affect the mechanical behavior of an epoxy-based nanocomposite. The weight percentage of a hardener is another important factor in the preparation of epoxy/thermoplastic/nanoparticle samples. Although the choice of an appropriate amount of this component is based on the stoichiometric ratio, effect is quite substantial, especially in the presence of the thermoplastic phase as a toughening agent as well as a nanofiller in epoxy resin, thus, the probability of

thorough mixing of epoxy monomers and the hardener would be dramatically decreased and hence prevent from complete polymerization. Mirmohseni et al. [12] determined an optimum amount of the hardener from the maximum tensile and impact strength values of epoxy samples. This optimization is called OVAT (one variable at a time) [30]. Leardi [30] claimed that 93% of the papers published in 2009 with general titles containing "optimization," "development," "improvement" or "effect of" employed the OVAT model. In many studies, optimized variables are totally dependent on each other, so their interaction should be determined, and OVAT cannot ensure finding a true optimum point [30]. In addition, prediction of nonlinear effects of each parameter is an important aspect that would require its determining via at least three points, which directly increase the number of experiments required for model prediction and consequently raises the costs. Central composite design (CCD), firstly introduced by Box and Wilson, is one of the extremely useful sequential second-order experimental designs to simultaneously decrease the number of experiments, predict possible nonlinear effects of each parameter and also their interaction [31]. After the construction of an appropriate mathematical model, one of the optimization methods should be used to predict the optimum values. Based on Charles Darwin's research in the 19th century, the genetic algorithm was worked out as a reliable method for solving complex problems [32]. Many researchers used this method to optimize complex studies in engineering [32–34]. The genetic algorithm is a global optimization method, which resresents design variables as individual genes or chromosomes [33]. Based on this algorithm, the result is stighily associated with its own problem. This method can find an answer to the wide range of problems and can govern a large number of versions at the same time. This trait reduces the probability that the algorithm is being restrieted to the local optimum points. This algorithm is easily applied to solving problems that have a large number of variables. The genetic algorithm is simple and does not require additional information, like a derivative of the objective function, to optimize complicated objective functions, discontinuous or non-differentiable functions or systems having no specific mathematical definition [32].

The main object of the present study is to introduce an epoxy-based nanocomposit with a new combination of components to simultaneously increase strength properties and toughness. It should be noted that in our previous study [3], the effect of adding a combination of thermoplastic and particulate nanofiller phases to an epoxy-based nanocomposite to simultaneously enhance tensile strength and damping properties in the first and second modes was investigated. In the current work, for improving mechanical properties, viz. flexural, compression and impact strength, thermoplastic [high impact polystyrene (HIPS)] and particulate nanofiller (silica) were added to the epoxy matrix. Central composite design is employed to present a model for predicting the mechanical behavior of the new nanocomposite. Based on the mathematical function obtained from CCD, the genetic algorithm is employed to find the optimum versions. The authors also tried to use inorganic nanofillers and commercial thermoplastics to reduce the total costs of sample preparation and concurrently achieve a considerable enhancement of mechanical properties. Morphological and structural characteristics of the hybrid mechanism are investigated with energy-dispersive X-ray (EDX) spectroscopy and scanning electron microscopy (SEM).

1. Experimental.

1.1. ***Materials and Sample Preparation***. All the materials employed in this study and also all the procedures used for sample preparation are detailed in [3].

1.2. ***Description.*** Flexural strength was determined in 3-point bending tests according to ASTM D790. These test methods cover the evaluation of flexural properties of reinforced plastics, including high-modulus composites. The specimen sizes were $127 \times 12.7 \times 3.2$ mm with a support span-to-depth ratio of 16. Compression tests were performed according to ASTM D695. Specimen sizes are $12.7 \times 12.7 \times 25.4$ mm. All of these mechanical tests are conducted on an STM-150 universal testing machine from Santam Company (Iran) with a load capacity of 150 kN. The impact strength was measured on unnotched specimens with the dimensions of 63.5, 12.7, and 7.2 mm as indicated in ASTM D256 using an SIT-50 Izod impact machine from Santam Company (Iran). At least five replicates for each sample were tested. A scanning electron microscope (SEM 1530) from TECNAN was employed to detect the dispersion of fracture surfaces of cured composites. The fracture surface was gold-coated prior to SEM studies to avoid charging and examined at 15 kV accelerating voltage.

1.3. ***Experiment of Design.*** The basic concept of the central composite model as experiment design is detailed in [3]. The input variables investigated were HIPS, SiO_2, and hardener contents. The actual and coded levels of design parameters are summarized in Table 1.

Table 1

Actual and Coded Levels of Design Parameters

Factors	Levels			Star points $\alpha = 1.68179$	
	Low (−1)	Central (0)	High (+1)	$-\alpha$	$+\alpha$
(X_1) HIPS content (wt.%)	4.0	7.0	10.0	2	12
(X_2) SiO_2 content (wt.%)	2.8	5.5	8.2	1	10
(X_3) hardener content (Phr)	23.0	26.0	29.0	21	13

2. Results and Discussion.

2.1. ***Statistical Modeling***. As mentioned above, to reduce the number of experiments, construct the mathematical model and finally optimize the results based on the CCD method, the results of compression, flexural, and impact tests are presented in Table 2. The important aspect is that each measurement is repeated five times and average values are reported in Table 2. STATISTICA software was used for predicting results, and the following equations were proposed:

$$Y_1 = 4.687 - 1.032(X_1) - 0.465(X_1)^2 - 0.605(X_2) - 0.712(X_2)^2 + 0.603(X_3) -$$

$$- 0.199(X_3)^2 + 0.112(X_1X_2) + 0.212(X_1X_3) + 0.012(X_2X_3), \qquad (1)$$

$$Y_2 = 192.551 - 40.512(X_1) - 15.179(X_1)^2 - 11.529(X_2) - 13.765(X_2)^2 +$$

T a b l e 2

Experimental Design and Corresponding Results

Run No.	Experimental factors (coded value)			Results of mechanical tests		
	HIPS content	SiO_2 content	Hardener content	Flexural strength (MPa)	Compression strength (MPa)	Impact strength (kJ/m^2)
1 (C)	0	0	0	4.50± 0.55	196± 22	47± 5
2	−1.68179	0	0	5.20± 0.83	222± 13	48± 1
3	−1.00000	1.00000	1.00000	4.10± 0.42	201± 5	47± 2
4	1.00000	1.00000	1.00000	2.60± 0.39	163± 26	31± 8
5 (C)	0	0	0	4.90± 0.28	190± 18	46± 3
6	−1.00000	−1.00000	1.00000	5.30± 0.15	237± 5	49± 2
7	1.00000	1.00000	−1.00000	1.20± 0.66	58± 29	37± 4
8	0	0	−1.68179	3.00± 0.64	120± 14	43± 2
9	0	1.68179	0	1.60± 0.93	136± 21	41± 3
10	−1.00000	−1.00000	−1.00000	4.80± 0.11	188± 11	48± 2
11	1.00000	−1.00000	−1.00000	2.00± 0.66	80± 16	33± 8
12	0	−1.68179	0	3.60± 0.52	166± 12	41± 2
13	0	0	1.68179	5.10± 0.35	200± 3	43± 3
14	1.00000	−1.00000	1.00000	3.80± 0.21	168± 8	31± 5
15	1.68179	0	0	1.40± 0.87	72± 15	26± 7
16	−1.00000	1.00000	−1.00000	3.10± 0.24	144 ± 17	43± 2

Note. C is the central point.

$$+31.745(X_3)-10.583(X_3)^2+6.625(X_1X_2)+10.875(X_1X_3)+3.125(X_2X_3), \quad (2)$$

$$Y_3 = 46.508-6.736(X_1)-3.378(X_1)^2-0.219(X_2)-1.964(X_2)^2-$$

$$-0.22(X_3)-1.257(X_3)^2+1.375(X_1X_2)-1.625(X_1X_3)-0.125(X_2X_3), \quad (3)$$

where Y_1, Y_2, and Y_3 are the ultimate flexural strength (UFS), ultimate compression strength (UCS), and impact strength (IS) of an epoxy-based ternary nanocomposite, respectively. At this stage, to demonstrate the validity of each parameter, the ANOVA tables presented in Table 3 were employed. Based on ANOVA results, the confidence limit determined at a 95% level and the significance of each part of the model were evaluated by their probability (*P*-value). If the terms have a significant effect on the result, the probability value will be less than 0.05 and the null hypothesis (H_0) will be rejected [35], and if the terms have no significant effect (i.e., with the *P*-value higher than 0.05), they would be eliminated from the final equation of the model. The results that illustrate

Table 3

Analysis of Variance for Central Composite Design Models

Function of responce		Source of variation									Error	Total – SS
		X_1	X_1^2	X_2	X_2^2	X_3	X_3^2	X_1X_2	X_1X_3	X_2X_3		
Y_1 (UFS)	Sum of squares	14.53856	2.00099	5.00019	4.69955	4.96175	0.36903	0.10125	0.36125	0.00125	0.33305	30.57750
	Df[1)]	1	1	1	1	1	1	1	1	1	6	15
	Mean square	14.53856	2.00099	5.00019	4.69955	4.96175	0.36903	0.10125	0.36125	0.00125	0.05551	–
	F-value[2)]	261.9163	36.0485	90.0798	84.6637	89.3874	6.6482	1.8240	6.5080	0.0225	–	–
	P-value	0.000004	0.000961	0.000078	0.000093	0.000080	0.041858	0.225543	0.043427	0.885632	–	–
Y_2 (UCS)	Sum of squares	22414.13	2134.51	1815.33	1755.30	13763.05	1037.57	351.12	946.13	78.12	935.93	43100.44
	Df	1	1	1	1	1	1	1	1	1	6	15
	Mean square	22414.13	2134.51	1815.33	1755.30	13763.05	1037.57	351.12	946.13	78.12	155.99	–
	F-value	143.6912	13.6838	11.6376	11.2528	88.2313	6.6516	2.2510	6.0654	0.5008	–	–
	P-value	0.000020	0.010098	0.014294	0.015333	0.000083	0.041822	0.184199	0.048934	0.505678	–	–
Y_3 (IS)	Sum of squares	619.7545	105.7361	0.6600	35.7408	0.6590	14.6393	15.1250	21.1250	0.1250	7.9500	775.7500
	Df	1	1	1	1	1	1	1	1	1	6	15
	Mean square	619.7545	105.7361	0.6600	35.7408	0.6590	14.6393	15.1250	21.1250	0.1250	1.3250	–
	F-value	467.7374	79.8005	0.4974	26.9741	0.4974	11.0485	11.4150	15.9433	0.0943	–	–
	P-value	0.000001	0.000110	0.507000	0.002027	0.507102	0.015926	0.014883	0.007177	0.769113	–	–

Note. [1)] Degree of freedom. [2)] Test for comparing the model variance and residual (error) variance.

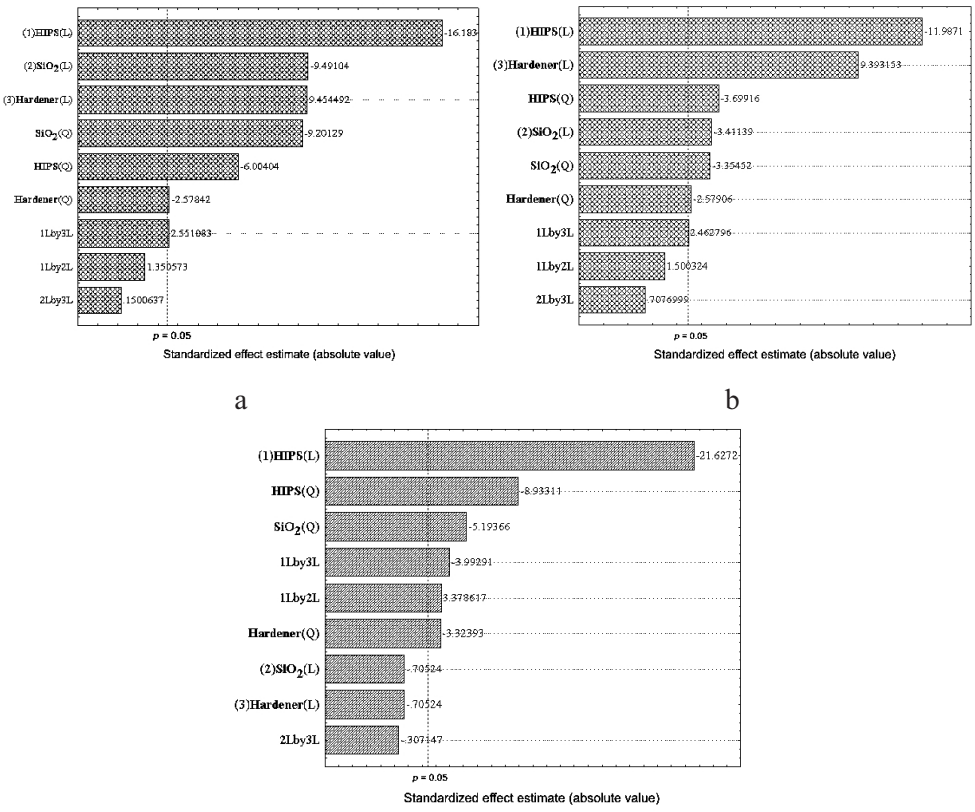

Fig. 1. Pareto charts of standardized effects: (a) flexural; (b) compression; (c) impact.

the effective or ineffective terms are presented in the format of Pareto charts and shown in Fig. 1. After determining the effective terms, Eqs. (1)–(3) are reduced to the following form:

$$\hat{Y}_1 = 4.687 - 1.032(X_1) - 0.465(X_1)^2 - 0.605(X_2) - 0.712(X_2)^2 + \\ + 0.603(X_3) - 0.199(X_3)^2 + 0.212(X_1X_3), \quad (4)$$

$$\hat{Y}_2 = 192.551 - 40.512(X_1) - 15.179(X_1)^2 - 11.529(X_2) - 13.765(X_2)^2 + \\ + 31.745(X_3) - 10.583(X_3)^2 + 10.875(X_1X_3), \quad (5)$$

$$\hat{Y}_3 = 46.508 - 6.736(X_1) - 3.378(X_1)^2 - 1.964(X_2)^2 - 1.257(X_3)^2 + \\ + 1.375(X_1X_2) - 1.625(X_1X_3). \quad (6)$$

Another criterion for evaluating the ability of the reduced model to predict the results is the coefficient of determination. However, the closer this value to 100%,

the more accurate estimate can be obtained. The data for each model, including predicted–observed diagrams, are shown in Fig. 2. With STATISTICA software, the 3D and contour graphs characterizing the mechanical behavior of a nanocomposite against variable parameters are depicted in Figs. 3–5.

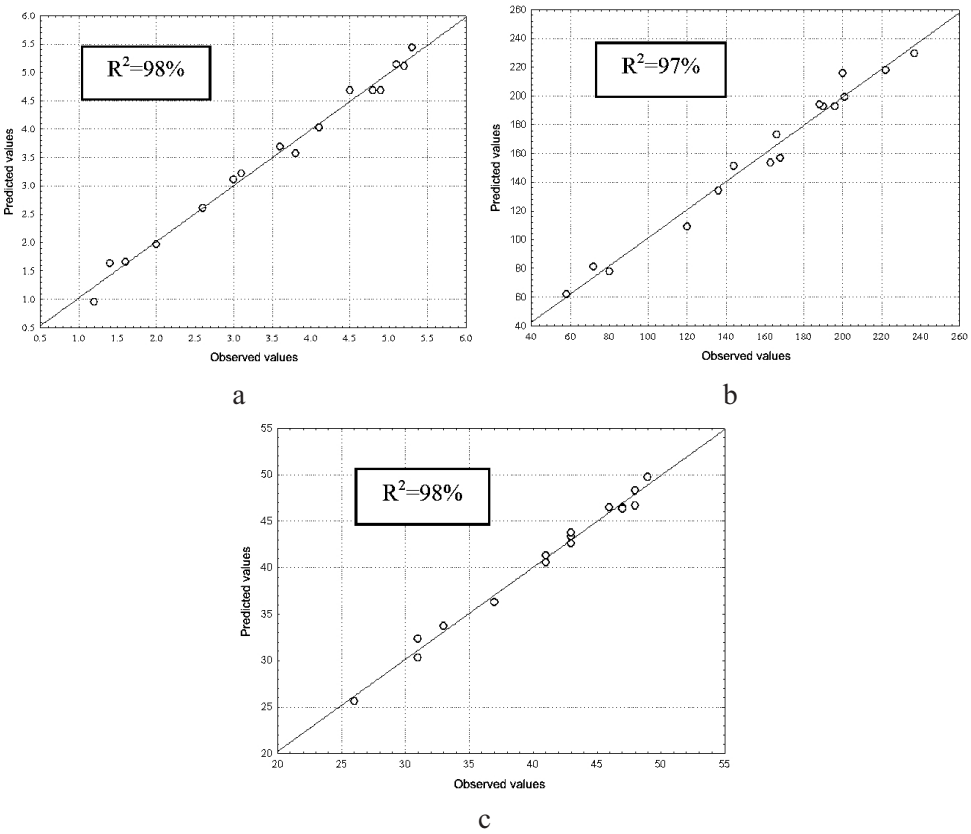

Fig. 2. Predicted vs observed data for flexural (a), compression (b), and impact (c).

2.2. ***Optimization of Mechanical Properties***. One of the main goals of the current study is to obtain and optimize the factors providing the best composition of a new hybrid epoxy-based nanocomposite. After constructing the final mathematical model for each mechanical property, the authors employed the genetic algorithm via the Matlab software to find the optimum conbination of components. The basic idea and algorithm details used to achieve the optimum combination for each parameter are given in [3]. Considering the above algorithm, to achieve the maximum mechanical properties, the optimum conditions were found as follows: for the ultimate tensile strength, a HIPS content of 4.54%, SiO_2 content of 4.15%, and hardener content of 28.6 phr, for the ultimate flexural strength, 4.39% of HIPS, 4.37% of nanosilica, and 29 phr of the hardener. The optimum values for the ultimate compression strength are 4.46% for HIPS, 4.42% for nanosilica and 29 phr for the hardener. Finally, the best levels of the modifiers and hardener for impact strength are 3.15% for HIPS, 4.28% for nanosilica and 28.4% phr for the hardener. The maximum values of mechanical properties predicted with this model at the optimum values of variables were: 69.8 MPa for UTS [3],

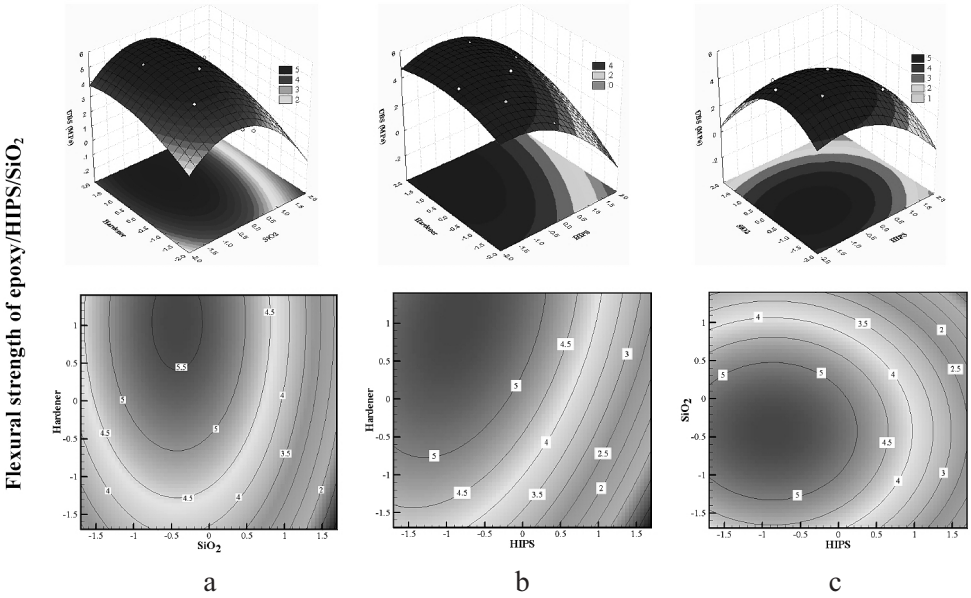

Fig. 3. 3D and contour plots of UFS at HIPS $= -0.87$ (a), $SiO_2 = -0.42$ (b), hardener $= 1$ (c).

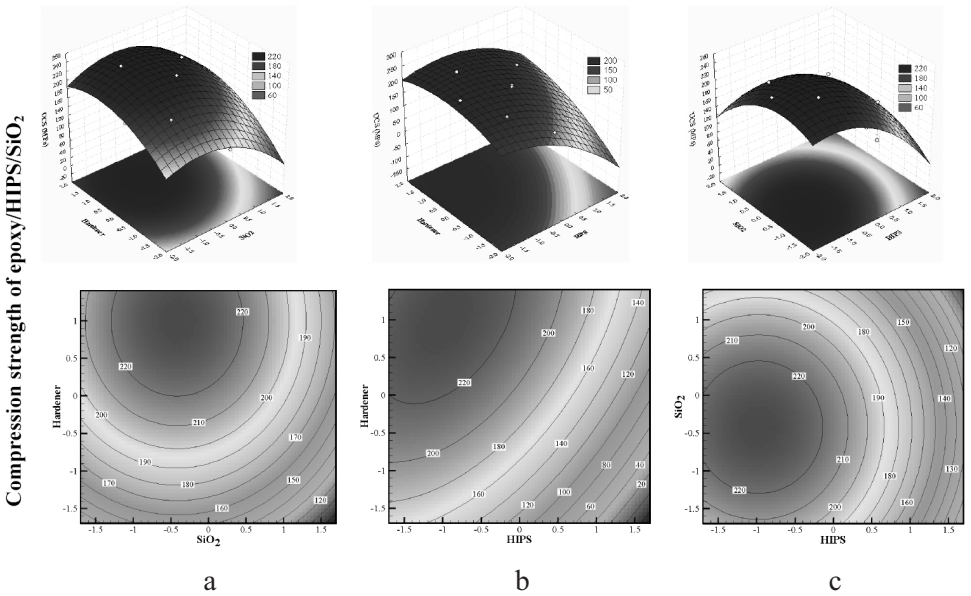

Fig. 4. 3D and contour plots of UCS at HIPS $= -0.98$ (a), $SiO_2 = -0.42$ (b), hardener $= 1$ (c).

5.58 MPa for UFS, 230 MPa for compression and 51 kJ/m^2 for impact strength. This survey was validated by preparing and testing the samples obtained under the optimum conditions. With five replications for each experiment, the following average results were obtained: 68.5 MPa for UTS, 5.67 MPa for UFS, 241 MPa for UCS, and finally 48 kJ/m^2 for impact strength. The examination of results demostrated that real values were in good agreement with those predicted by the model. Moreover, as the previous studies confirm, the simutaneous addition of

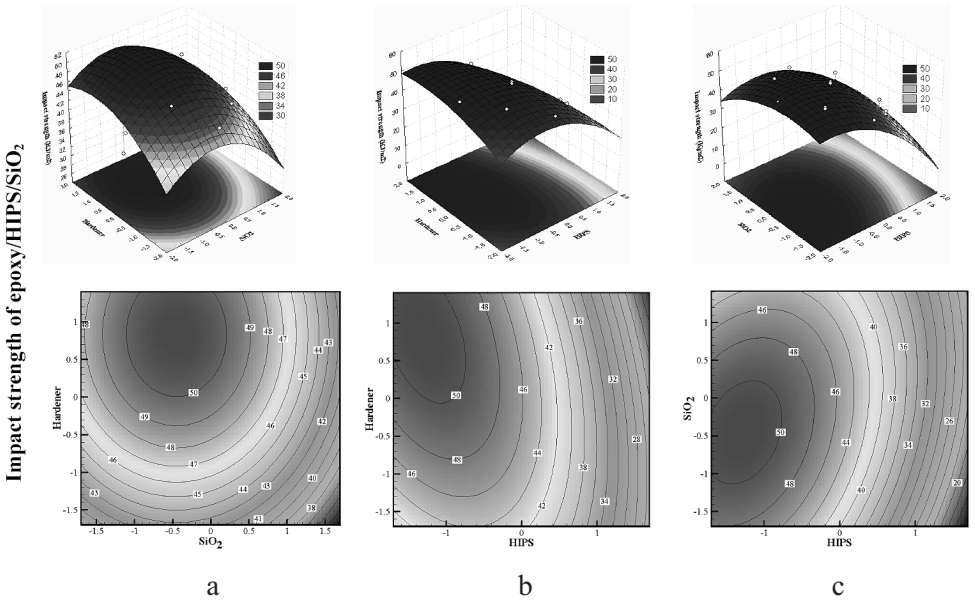

Fig. 5. 3D and contour plots of IS at HIPS $= -1.29$ (a), $SiO_2 = -0.45$ (b), hardener $= 0.83$ (c).

nano- and thermoplastic phases to epoxy resin can lead to different results. Assef et al. [35] reported that clay and polyetheretherketone dramatically decrease the impact strength. Baker et al. [36] showed that with adding 2% clay and 20% polyamide, the impact strength would be enhanced up to 115%. Mirmohseni et al. [37] demonstrate that with the incorporation of 2.5% clay nanoparticles and 4 phr ABS into the epoxy matrix, a 133% improvement was observed for the impact strength.

2.3. ***3D and Contour Plots for the Mechanical Behavior of an Epoxy-Based Hybrid Nanocomposite***. In this study, for demonstrating the relation between the mechanical properties of an epoxy-based hybrid nanocomposite and the effective parameters as design factors, the 3D response surface and contour plots were employed.

2.3.1. *Effect of the Hardener and Silica Loading on Mechanical Properties*. Figures 3a, 4a, and 5a present the 3D response surface and 2D contour plots of flexural, compression and impact strength of epoxy/HIPS/SiO_2 ternary nanocomposite as a function of hardener and silica nanoparticles contents, while the HIPS factor was at its optimum concentration for each property. As it is obvious from the results, in similar cases the silica and hardener loading exert a significant effect on examined mechanical properties. The flexural, compression and impact strength increased with growing silica contents to some extent and decreased with higher loadings. This amount varied within 4.0–4.5%. As Mirmohseni et al. reported [35], the best concentration of hardener for the hybrid mechanism may not occur at a stoichiometric ratio (23 phr) and the optimum loading for the hardener is between 28–29 phr. It can also be concluded that the interaction of the hardener and silica nanoparticles have an insignificant effect on the results. It can be explained by the fact that due to small sizes and low concentrations of silica nanoparticles, they cannot prevent good hardener performance in polymerization of epoxy monomers.

2.3.2. *Effect of the Hardener and HIPS Loading on the Mechanical Properties*. Figures 3b, 4b, and 5b show the response surface and contour plots for demonstrating the hardener and HIPS effects on the flexural, compression and impact strength values of an epoxy/HIPS/silica hybrid nanocomposite. In these figures the SiO_2 loading is fixed at its best concentration for each property. As is seen, the hardener behavor is the same as in the previous section. The main processing defects in epoxy-based nanocomposites seem to be related to entrained voids and incomplete cure during the cross-linking phase. Notice that the HIPS loading results in the optimum mechanical strength at different contents. The optimum amount of HIPS for tensile strength [3] is 4.54%, for flexural strength is 3.19%, for compressive strength is 4.1%, and finally for impact strength is 3.15%. According to the obtained results, a considerable effect of the HIPS–hardener interaction is observed. This behavior can be explained by large sizes of HIPS particles that prevent from the complete involvement of epoxy monomers by the hardener and decrease the chance of all epoxy monomers to participate in polymerization.

2.3.3. *Effect of the HIPS and SiO_2 Loading on the Mechanical Properties*. The effect of HIPS and nano-SiO_2 contents on mechanical strength of an epoxy-based nanocomposite is depicted in Figs. 3c, 4c, and 5c. As was mentioned above, these factors have a significant influence on the results. Thermoplastic particles increase the fracture toughness due to the shear bonding and dilation of the matrix from the plastic zone an the crack tip [6, 7, 40, 41]. A localized plastic zone at the crack tip can modify the stress field, limiting high local stresses and thereby reducing the probability of crack growth. This strategy can also lead to the absorption of more energy than it would be required for the equivalent growth of a brittle crack. Here, with no account of tension, compression and flexure, interaction between HIPS and SiO_2 has a significant effect on the impact strength. This behavior may be associated with the fact that, in the presence of HIPS and SiO_2, viscosity increases, while the possibility of getting a homogeneous mixture decreases. This may lead to the agglomeration of SiO_2 nanoparticles and formation of large particles, which cannot transfer the energy of impact in all materials. In addition, this nonuniform distribution of nanoparticles generates stress concentrations becoming the origin of cracks that decreases the impact strength. As is seen in Fig. 6, HIPS alone would considerably decrease the tensile and flexural strength values and would have a negligible positive effect on the compression of the epoxy matrix at low concentrations. It can be found from Fig. 6a that in a ternary nanocomposite, the ultimate tensile strength and elongation at break increased up to 69 and 265% respectively [3]. As is seen in Fig. 6b, the flexural strength of a hybrid nanocomposite in comparison with "neat" (i.e., pure) epoxy sample decreased by 5%. The elongation at break increased up to 144% (see Figs. 6b and 7). It can also be found that at the addition of thermoplastic or nanoparticle phases, the flexural modulus exhibits a general tendency to decrease. The ultimate compression strength increased up to 57% and the compression strain did not change considerably (Fig. 6c). The impact strength of an epoxy/HIPS/SiO_2 ternary nanocomposite at the optimum HIPS, silica, and hardener contents increased up to 421%. This demostrates the synergistic effect of silica and HIPS modifiers on the impact strength of a hybrid nanocomposite. It is clear that the addition of rigid nanoparticles (silica)

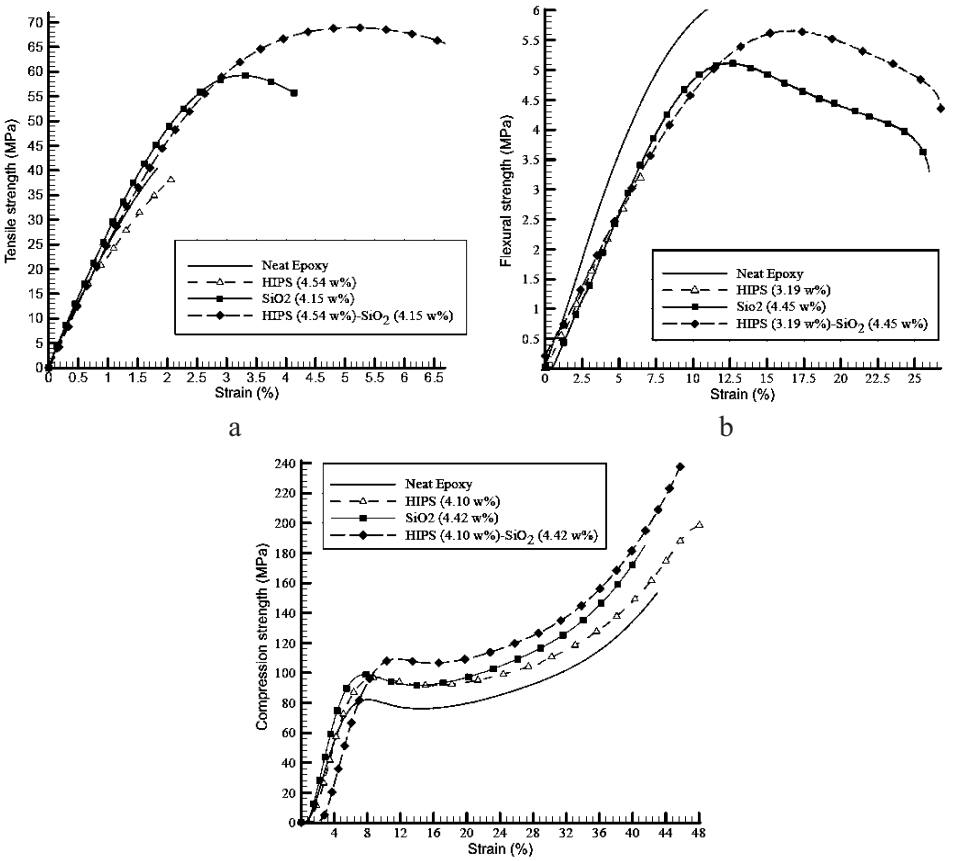

Fig. 6. Stress–strain plots: tensile (a), flexural (b), and compression (c).

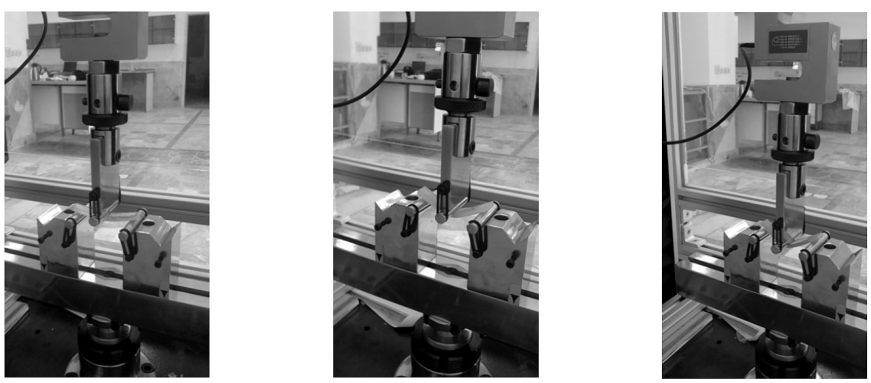

Fig. 7. Elongation before the break moment under flexural loading for "neat" epoxy (a), epoxy/(4.45 wt.% SiO_2) (b), and (c) epoxy/(3.19 wt.% HIPS)/(4.45 wt.% SiO_2) (c).

enhances the mechanical properties (Fig. 6). The addition of HIPS as a thermoplastic phase increased the elongation (Figs. 6 and 7). The simultaneous addition of HIPS as a thermoplastic modifier and silica as a nanoparticulate material can considerably improve the mechanical strength and fracture toughness (Figs. 6 and 7).

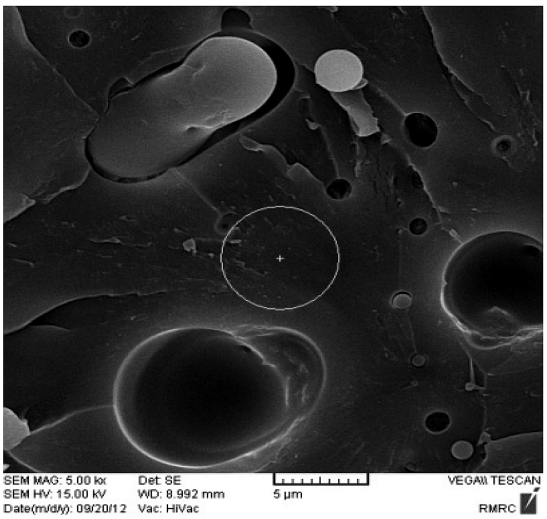

a

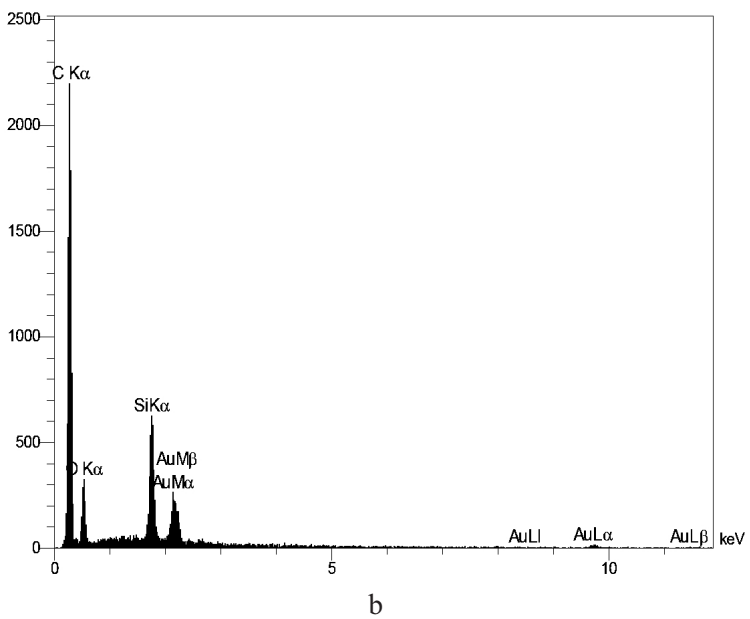

b

Fig. 8. SEM (a) and EDX (b) micrographs for epoxy/HIPS/SiO_2.

The micrograph shows the cut-off surface of a tensile specimen at the optimum HIPS, SiO_2, and hardener amounts (Fig. 8) obtained in [3]. In epoxy materials, the cross-link density plays a vital role in achieving a good mechanical properties. As is seen, a good dispersion of silica nanoparticles and high-impact polystyrene as a thermoplastic phase with small agglomeration occurred. The phase separation of nano- and microparticles in the epoxy-rich matrix was observed. This modifier with homogenous dispersion can be of importance for the crack arrest and reinforcement in enhancing the mechanical strength [40, 41]. SEM and EDX studies of epoxy/HIPS/SiO_2 samples showed the uniform distribution of silica nanoparticles in the matrix (Fig. 8).

Conclusions. In the current study, the new combination of a thermoplastic nanofiller as a modifier for an epoxy-based composite has been proposed. Tensile, flexural, compressive, and impact strength values are four decisive mechanical properties that have been studied. The central composite model as an experiment design was employed to predict and optimize the results. Also the genetic algorithm was used to optimize the models provided by CCD. The effect of different parameters on the mechanical strength of an epoxy/HIPS/SiO_2 ternary nanocomposite is also represented by the 3D response surface and 2D contour plots. It was found that the combination of HIPS and silica nanoparticles significantly increased the tensile, compressive, and impact strength values of epoxy resin up to 69, 57, and 421%, respectively. Although the flexural strength did not change positively, the elongation at break for tensile and flexural samples increased up to 265 and 144%, respectively. Correlation between morphology and mechanical properties was obtained with SEM and EDX techniques.

Р е з ю м е

Незважаючи на те що епоксидні смоли мають хорошу границю міцності при розтязі, вони крихкі і характеризуються слабким опором розвитку тріщини. Із метою покращання механічної міцності і в'язкості руйнування епоксидних нанокомпозитів як модифікатор використовували новий комбінований термопластичний дисперсний наповнювач. До складу отриманого трикомпонентного епоксидного нанокомпозита входить ударостійкий полістирол у вигляді термопластичних і кремнеземних наночастинок, що являють собою його дисперсні фази. Щоб отримати більш високі показники міцності без впливу на інші задані механічні показники, проводили випробування на міцність при згині і стиску та на ударну в'язкість. Для представлення математичних моделей з метою прогнозування механічної поведінки гібридного нанокомпозита як функцію фізичних чинників використали центральний композиційний план. Досліджували вміст ударостійкого полістиролу, кремнезему і зміцнювального елемента в нанокомпозиті. На основі математичних функцій, отриманих за моделлю центрального композиційного плану, для виведення оптимальних значень механічних властивостей використовували генетичний алгоритм, що є одним із найміцніших засобів оптимізації. Установлено, що поєднання наночастинок на основі ударостійкого полістиролу і кремнезему збільшує опір епоксидної смоли стиску на 57%, удару – на 421%. У той же час позитивних змін при опорі згину не відмічається, видовження за згинального розриву збільшується до 144%. Проведено дослідження морфології поверхні руйнування за допомогою енергодисперсійного випромінювання і сканувальної електронної мікроскопії.

1. M. M. Shokrieh, M. A. Torabizadeh, and A. Fereidoon, "A new method for evaluation of mechanical properties of glass/epoxy composites at low temperatures," *Strength Mater*., **44**, No. 1, 87–99 (2012).
2. M. M. Shokrieh, M. A. Torabizadeh, and A. Fereidoon, "Progressive failure analysis of glass/epoxy composites at low temperatures," *Strength Mater*., **44**, No. 3, 314–324 (2012).

3. Y. Rostamiyan and A. B. Fereidoon, "Preparation, modeling, and optimization of mechanical properties of epoxy/HIPS/silica hybrid nanocomposite using combination of central composite design and genetic algorithm. Part 1. Study of damping and tensile strengths," *Strength Mater*., **45**, No. 5, 619–634 (2013).
4. T. H. Hsieh, A. J. Kinloch, K. Masania, et al., "The mechanisms and mechanics of the toughening of epoxy polymers modified with silica nanoparticles," *Polymer*, **51**, 6284–6294 (2010).
5. E. H. Rowe, A. R. Siebert, and R. S. Drake, "Toughening thermosets with butadiene/acrylonitrile polymers," *Mod. Plast*., **47**, 110–117 (1970).
6. A. J. Kinloch, S. J. Shaw, D. A. Tod, and D. L. Hunston, "Deformation and fracture behaviour of a rubber-toughened epoxy: 1. Microstructure and fracture studies," *Polymer*, **24**, Issue 10, 1341–1354 (1983).
7. R. A. Pearson and A. F. Yee, "Toughening mechanisms in elastomer-modified epoxies," *J. Mater. Sci.*, **21**, 2475–2488 (1986).
8. A. J. Kinloch, M. L. Yuen, and S. D. Jenkins, "Thermoplastic-toughened epoxy polymers," *J. Mater. Sci*., **29**, 3781–3790 (1994).
9. R. D. Brooker, A. J. Kinloch, and A. C. Taylor, "The morphology and fracture properties of thermoplastic-toughened epoxy polymers," *J. Adhes*., **86**, Issue 7, 726–741 (2010).
10. N. G. Yun, Y. G. Won, and S. C. Kim, "Toughening of epoxy composite by dispersing polysulfone particle to form morphology spectrum," *Polym. Bull*., **52**, 365–372 (2004).
11. M. Kimoto and K. Mizutani, "Blends of thermoplastic polyimide with epoxy resin: Pt. II. Mechanical studies," *J. Mater. Sci*., **32**, 2479–2483 (1997).
12. A. Mirmohseni and S. Zavareh, "Preparation and characterization of an epoxy nanocomposite toughened by a combination of thermoplastic, layered and particulate nano-fillers," *Mater. Des*., **31**, No. 6, 2699–2706 (2010).
13. K. Mimura, H. Ito, and H. Fujioka, "Improvement of thermal and mechanical properties by control of morphologies in PES-modified epoxy resins," *Polymer*, **41**, Issue 12, 4451–4459 (2000).
14. L. R. F. Rose, "Toughening due to crack-front interaction with a second-phase dispersion," *Mech. Mater*., **6**, Issue 1, 11–15 (1987).
15. K. T. Faber and A. G. Evans, "Crack deflection processes – II. Experiment," *Acta Metall*., **31**, No. 4, 577–584 (1983).
16. J. Lee and A. F. Yee, "Inorganic particle toughening I: Micro-mechanical deformations in the fracture of glass bead filled epoxies," *Polymer*, **42**, No. 2, 577–588 (2001).
17. J. Lee and A. F. Yee, "Inorganic particle toughening II: Toughening mechanisms of glass bead filled epoxies," *Polymer*, **42**, No. 2, 589–597 (2001).
18. J. Lee and A. F. Yee, "Fracture of glass bead/epoxy composites: on micro-mechanical deformations," *Polymer*, **41**, Issue 23, 8363–8373 (2000).

19. T. Kawaguchi and R. A. Pearson, "The effect of particle–matrix adhesion on the mechanical behavior of glass filled epoxies. Pt. 2. A study on fracture toughness," *Polymer*, **44**, Issue 15, 4239–4247 (2003).
20. C. Roscher, "Tiny particles, huge effect: Radiation curable silica nanocomposites for scratch and abrasion resistant coatings," *Eur. Coat. J.*, No. 4, 138–142 (2003).
21. R. A. Vaia, T. Benson Tolle, G. F. Schmitt, et al., "Nanoscience and nanotechnology: materials revolution for the 21st century," *SAMPE J.*, **37**, 4–31 (2001).
22. E. T. Thostenson, C. Li, and T.-W. Chou, "Nanocomposites in context," *Compos. Sci. Technol*., **65**, 491–516 (2005).
23. B. Wetzel, F. Haupert, K. Friedrich, et al., "Impact and wear resistance of polymer nanocomposites at low filler content," *Polymer Eng. Sci*., **42**, Issue 9, 1919–1927 (2002).
24. H. Zou, S. Wu, and J. Shen, "Polymer/silica nanocomposites: preparation, characterization, properties, and applications," *Chem. Rev*., **108**, 3893–3957 (2008).
25. H. Zhang, L. A. Berglund, "Deformation and fracture of glass bead/CTBN-rubber/epoxy composites," *Polymer Eng. Sci.*, **33**, Issue 2, 100–107 (1993).
26. J. Lee and A. F. Yee, "Micro-mechanical deformation mechanisms in the fracture of hybrid-particulate composites based on glass beads, rubber and epoxies," *Polymer Eng. Sci.*, **40**, Issue 12, 2457–2470 (2000).
27. F. Ravari, A. Omrani, A. A. Rostami, and M. Ehsani, "Ageing effects on electrical, morphological, and mechanical properties of a low viscosity epoxy nanocomposite," *Polymer Degrad. Stab*., **97**, No. 6, 929–935 (2012).
28. A. Omrani, L. C. Simon, A. A. Rostami, and M. Ghaemy, "Cure kinetics, dynamic mechanical and morphological properties of epoxy resin–Im6NiBr2 system," *Eur. Polymer J*., **44**, No. 3, 769–779 (2008).
29. A. Omrani, L. C. Simon, and A. A. Rostami, "Influences of cellulose nanofiber on the epoxy network formation," *Mater. Sci. Eng. A*, **490**, 131–137 (2008).
30. R. Leardi, "Experimental design in chemistry: a tutorial," *Anal. Chim. Acta*, **652**, 161–172 (2009).
31. P. Angelopoulos, H. Evangelaras, and C. Koukouvinos, "Small, balanced, efficient and near rotatable central composite designs," *J. Statist. Plan. Infer.*, **139**, No. 6, 2010–2013 (2009).
32. J. S. Chung and S. M. Hwang, "Application of a genetic algorithm to the optimal design of the die shape in extrusion," *J. Mater. Process. Technol*., **72**, No. 1, 69–77 (1997).
33. R. G. Song and Q. Z. Zhang, "Heat treatment optimization for 7175 aluminum alloy by genetic algorithm," *Mater. Sci. Eng. C*, **17**, Issues 1-2, 133–137 (2001).
34. R.-G. Song, Q.-Z. Zhang, M.-K. Tseng, and B.-J. Zhang, "The application of artificial neural networks to the investigation of aging dynamics in 7175 aluminium alloys," *Mater. Sci. Eng. C*, **3**, Issue 1, 39–41 (1995).

35. A. Asif, K. Leena, V. Lakshmana Rao, and K. N. Ninan, "Hydroxyl terminated poly(ether ether ketone) with pendant methyl group-toughened epoxy clay ternary nanocomposites: preparation, morphology, and thermomechanical properties," *J. Appl. Polymer Sci.*, **106**, Issue 5, 2936–2946 (2007).
36. A. Mirmohseni and S. Zavareh, "Modeling and optimization of a new impact-toughened epoxy nanocomposite using response surface methodology," *J. Polymer Res.*, **18**, 509–517 (2011).
37. A. Mirmohseni and S. Zavareh, "Epoxy/acrylonitrile-butadiene-styrene copolymer/clay ternary nanocomposite as impact toughened epoxy," *J. Polymer Res.*, **17**, No. 2, 191–201 (2010).
38. Y. Huang and A. J. Kinloch, "Modelling of the toughening mechanisms in rubber-modified epoxy polymers," *J. Mater. Sci.*, **27**, Issue 10, 2763–2769 (1992).
39. A. F. Yee and R. A. Pearson, "Toughening mechanisms in elastomer-modified epoxies," *J. Mater. Sci.*, **21**, 2462–2474 (1986).
40. J. López, C. Ramirez, M. J. Abad, et al., "Blends of acrylonitrile–butadiene–styrene with an epoxy/cycloaliphatic amine resin: phase-separation behavior and morphologies," *J. Appl. Polymer Sci.*, **85**, Issue 6, 1277–1286 (2002).
41. Y. Müller, L. Häuβler, and J. Pionteck, "ABS-modified epoxy resins – curing kinetics, polymerization induced phase separation, and resulting morphologies," *Macromolec. Symp*., **254**, Issue 1, 267–273 (2007).

Received 12. 06. 2013